International Journal of Scientific Engineering and Research (IJSER)
www.ijser.in
ISSN (Online): 2347-3878
Volume 2 Issue 9, September 2014

Vibration Monitoring of Rotating Machines Using MEMS Accelerometer

Subimal Bikash Chaudhury[1], Mainak Sengupta[2], Kaushik Mukherjee[2]
1 Automation Division, Tata Steel, Jamshedpur, India,
2 Electrical Engineering, Indian Institute of Engineering Science & Technology, Shibpur, India

Abstract: ***Heavy industries face major problems since different types of mechanical failures can originate in rotating machines. Analytical approaches have demonstrated that vibration monitoring has tremendous potential in detecting and localizing defects in the machines. There are different technologies available for vibration sensing. Though MEMS accelerometer is slowly becoming an alternate method for vibration monitoring of rotating machines, yet it has not been fully explored for a much wider application base. This paper proposes the basic design for the development of a low cost MEMS accelerometer based vibration sensor by integrating the basic sensor and intelligence of vibration analysis, together. This module can easily be deployed for different rotating machines for vibration monitoring. Sensitivity of the sensor, effectiveness of the proposed intelligence in signal processing and their performance are tested for a 7.5KW, 3ϕ, 440V, 4 pole squirrel-cage induction motor. The experiments are carried out to check the ability to detect the fault frequency peaks under different fault combinations. The results presented here are found to be highly promising.***

Keywords: Rotating Machine, MEMS accelerometer, vibration sensor, autocorrelation function, fault diagnosis, signal processing

1. Introduction

The fault diagnosis and prognosis of a rotating machine using vibration pattern analysis, is one of the efficient and most successful techniques [1-3]. Analytical and practical understanding of machine vibration is well defined in literatures [2-5]. The machine vibration behavior, in time and frequency domain, forms the basis for monitoring of rotating machines [6]. It has gained enormous importance in the last decade, as machine vibration response is sensitive to any small change in operating condition or mechanical structural [2,4].

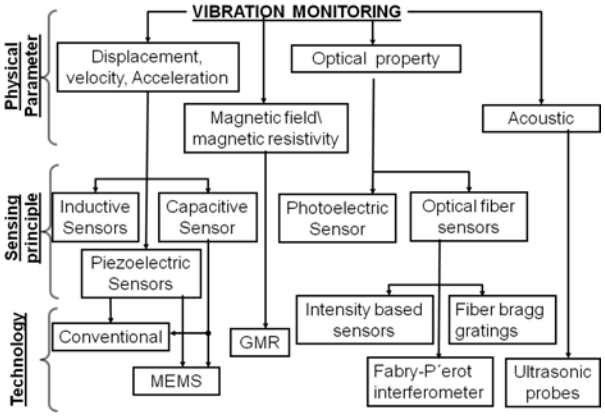

Figure 1: Overview of different vibration sensors and technologies used for vibration monitoring

The vibration analysis demands appropriate vibration transducers. Vibration measurement can be done by measuring displacement, velocity, acceleration, acoustic, magnetic, optical etc. of specific points, of otherwise static structure. These parameters can be measured with different types of sensing devices based on different principles. Several techniques, mainly based on capacitive/piezoelectric accelerometers and acoustic are available commercially. Optical [7,8] and GMR (Giant Magnetoresistance) [9] based vibration measurement are emerging technologies. Fig.-1 presents different physical parameters for vibration sensing, sensors adopted for sensing, and technologies available for vibration monitoring.

Out of the different technologies, MEMS accelerometers are projected to hold great promise for the future of smart vibration sensing [10]. Number of research studies exist in the literature [10,11] about MEMS accelerometer construction, mounting considerations, measurement principle and performance evaluation. These MEMS based accelerometers are emerging as an alternate method of sensing the vibration in rotating machines. Although MEMS technology is widely applied in biomedical, automotive and consumer sectors, yet there is a lack of rigorous investigation of MEMS accelerometers performance in vibration measurements under different operating and fault conditions of rotating machines.

The main objective of this work is to investigate the feasibility of MEMS accelerometer for vibration monitoring of mechanical equipments. The complete vibration transducer design aspects are detailed here. The influence of vibration noise in rotating machines is investigated, particularly when useful signal becomes hard to obtain. An auto-correlation based noise cancellation algorithm and adaptive rule-based filter are developed to improve the characteristic signal detection capability in the acceleration signal.

To experimentally verify the validity of the deign aspects of vibration transducer and the proposed signal processing technique, a series of laboratory tests were conducted. The test rig comprised mainly of the test motor with gear arrangement for load transfer and dynamometer. Different conditions were emulated for the motor and load arrangement, corresponding to different faults like shaft misalignment, motor misalignment, loose foundation, eccentric loading conditions etc.

This paper is organized as follows. In Section II, the basic principle of MEMS sensor is discussed. The design aspects of MEMS based vibration transducer and the complete development are discussed in Sections III and IV respectively.

The experimental results are presented in Section V. Finally conclusions are given in Section VI.

2. MEMS Accelerometer - Fundamentals

MEMS accelerometers are based on two sensing principles (1) piezoelectric effect – in which microscopic crystal gets stressed by accelerative forces, (2) capacitive type –where the capacitance changes between two fingers due to microscopic seismic mass movement [10-13]. In either case a voltage is generated which is the measure of force or displacement.

Capacitive type MEMS accelerometers [14, 15] are widely used since they need minimal processing power, produce a large output signal, have excellent sensitivity and are intrinsically insensitive to temperature variations. The sectional view and the simplified lumped parameter model for a capacitive type MEMS accelerometer is shown in Fig.-2(a,b).

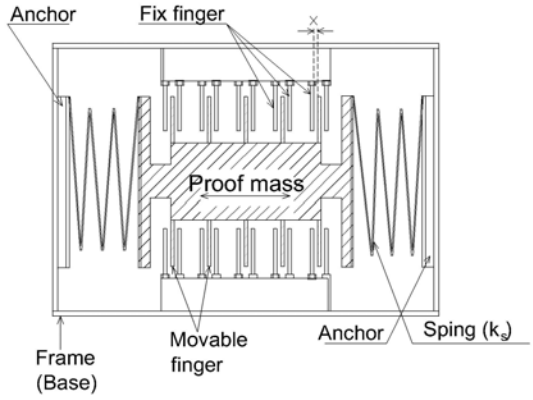

(a) Sectional view of MEMS accelerometer

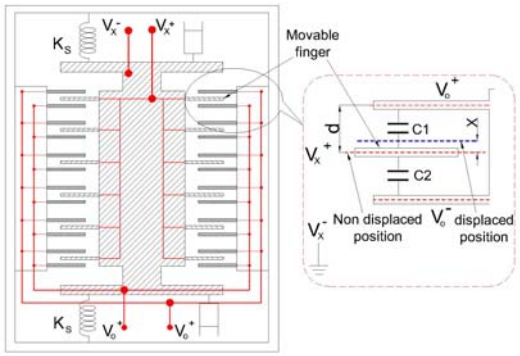

(b) Lumped parameter model

Figure 2: Capacitive type MEMS accelerometer

This type of sensor works on the principle of capacitance variation between a set of sensing electrodes and reference (fixed) electrodes. The capacitance between two parallel plates with 'A', as the area of each plate, and 'd', as the separation between the plates (Fig.-2b), can be given as:

$$C = \varepsilon_0 \varepsilon_r \frac{A}{D} \tag{1}$$

Where, ε_0 is the permittivity of free space and ε_r is the dielectric constant or relative permittivity of the insulator used. The acceleration is inferred from the displacement (x) of the proof mass 'm' (direction of arrow mark) and is measured using the change in the capacitance (ΔC) between the anchor and the electrodes. The force acting on the proof mass (= m x a) is balanced by the restoring force '= k_s x x' generated by the spring. Where k_s is the spring constant.

$$\therefore a = \frac{k_s}{m} x \tag{2}$$

Under no deflection condition:

$$C_1 = C_2 = C_0 \tag{3}$$

Under deflection:

$$C_1 = C_0 + \Delta C = \varepsilon_0 \frac{1}{d + x} \tag{4}$$
$$C_2 = C_0 - \Delta C = \varepsilon_0 \frac{1}{d - x}$$

Considering $x < d, \quad \therefore x^2 << d^2$

The voltage balance (based on charge conservation) for one set of capacitor bank can be considered as:

$$V_x = V_0 \frac{C_2 - C_1}{C_2 + C_1}$$

$$\frac{V_x}{V_0} = \frac{\Delta C}{C_0} = \frac{x}{d} \qquad \therefore x = d \frac{\Delta C}{C_0}$$

where, V_x , V_0 are sensed and applied voltages, respectively.

Solving (2), (6) and (7), acceleration can be defined as

$$a = \frac{k_s}{\underset{constant}{mV_0}} V_x \tag{8}$$

Equ.-(8) provides the basis of acceleration measurement.

3. Design Consideration

The bandwidth, noise characteristics and sensitivity of MEMS sensors are important parameters for selecting the MEMS and designing the circuit. Some of the design parameters are discussed here.

3.1 Bandwidth selection

The bandwidth of MEMS accelerometer gives the maximum input frequency for which the sensor will respond effectively. During frequency analysis of vibration signal, the appearance of prominent periodic frequency components is an indication of the machine condition [7, 8]. These frequencies are generally related to the rotational speed of various parts of the machine. For example if the rotational frequency appears as f_r, then the coupling misalignment will change the amplitude of f_r significantly, whereas, $2 \times f_r$ will change only in case of misaligned shafts. Similarly, gear mesh frequency $f_Z = n \times f_g$ where, n is number of gear teeth and f_g is gear rotating speed. These frequencies of interest are the deciding factors for selecting the required bandwidth of the sensor.

International Journal of Scientific Engineering and Research (IJSER)
www.ijser.in
ISSN (Online): 2347-3878
Volume 2 Issue 9, September 2014

Here, the design of MEMS accelerometer as vibration sensor is restricted to fault frequency identification for misaligned rotating shaft with speed ranging from few RPM to 3000RPM (50Hz). Hence, a device with low bandwidth (0-500Hz) is selected.

3.2 Signal pre-processing

Most of the MEMS accelerometer outputs and bias outputs (i.e. output at g = 0) are ratiometric. The DC-component which appears in the signals is either an artifact of the sensors and electronics associated with the hardware or it may be due to the low-speed operation of the motor. It is essential for the DC-component to be removed before conducting any frequency domain analysis. Moreover, to get the best resolution of ADC it is recommended to remove the bias voltage and amplify the signal with proper gain. It is proposed to carry out same using level-shifter with gain amplifier using instrument amplifier. Fig.- 3 shows the basic schematic of the amplifier considered for bias voltage removal and signal amplification.

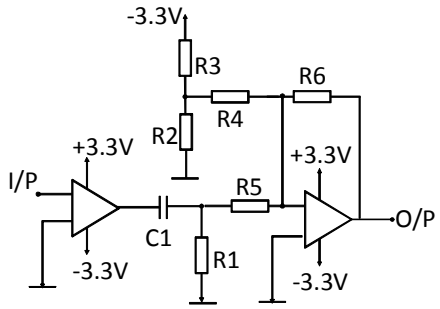

Figure 3: Schematic for signal preprocessing.

Further, a new concept is proposed to remove the residual DC component. The DC-component in the signal can be obtained as the amplitude of zero frequency component of the spectral decomposition (FFT) of continuous time series sensor signal x(t) . This is expressed here as,

$$X_{DC}^{F} = \tilde{X}_{0}^{F}$$

where,

X_{DC}^{F} represents the DC-component in digitized signal

$\tilde{X}_{0}^{F}$ is the zero frequency component obtained from FFT

F digitized frame number.

Each digitized frame $\hat{x}[k]$ captured from continuous time series signal $x(t)$ is corrected by subtracting the DC-component from the digitized frame. The reconstructed frame is:

$$\hat{X}^{F} = \left(\hat{x}[k] - \tilde{X}_{0}^{F}\right)$$

3.3 Noise consideration

The inherent noise of the accelerometer and the large amount of vibration noise which often originates in the floor area of the installation, need to be considered for recovering the desired signal from the accelerometer signal. The design aspect for removing both these types of noises is discussed in the subsequent paragraphs.

The inherent noise of MEMS has $1/f$ type noise characteristics at low frequencies and white Gaussian noise at high frequencies [17,18]. This is random in smaller time frames of the vibration signal with uncorrelated nature. Vibration signal from other sources can also be random but for longer time frame, non-persistent and at higher frequency band-width. The nature of this noise signal may be periodic or aperiodic. The aperiodic random signal appears as noise floor, which may vary depending on their randomness and amplitude. In the present design, the removal all of these unwanted signals is done via multiple steps- using spectral averaging, one-sided autocorrelation function and using rule based filter (using Spectral Subtraction).

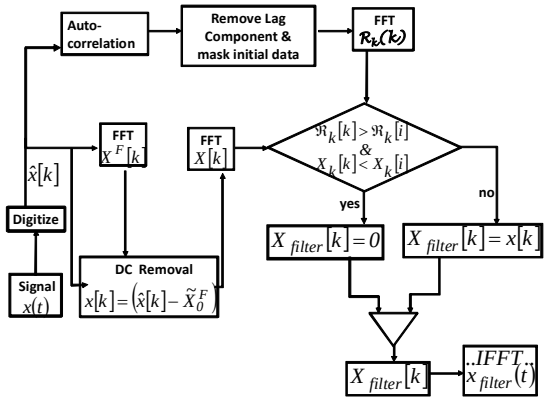

Figure 4: Annotation of different steps involved in denoising of vibration signal using Auto-correlation function

One of the important contributions of this paper is to propose, develop and implement logic for random noise removal using auto-correlation function. This is illustrated in Fig.-4.

3.4 Mounting requirement and orientation

The mounting and orientation of the basic MEMS sensor is very important. The orientation of MEMS is critical, since the measured acceleration is sensitive to a particular direction. The direction of acceleration which needs to be measured is dependent on the type of fault causing the vibration.

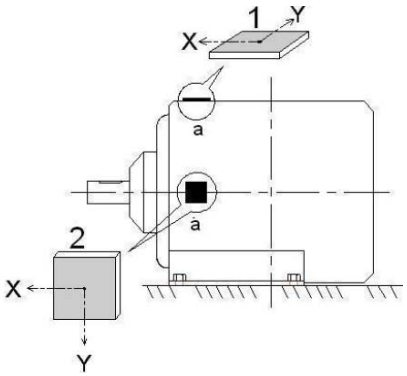

Figure 5: Schematic of the probable location for sensor fixing. (1) Y axis is along the perpendicular direction of gravitational force, (2) Y axis is along the gravitational force

For example, a shaft misalignment will have more prominent axial vibration, whereas radial vibration measurement will be more salient in the case of an imbalance in the machine. Two possible mounting locations 'a' and 'b' are indicated in Fig.-5. Although both these positions can be considered, the position 'b' is preferable since at this position the radial component will be more prominent and will provide a direct indication of the machine alignment. Here, in either position, x-axis of the MEMS is oriented towards the machine shaft axis (i.e. axial direction of motor). It is better to have the alignment of x-axis of the MEMS along the shaft axis of the motor, which will in turn give more accurate measurement.

4. Development of Vibration Transducer

Considering the vibration level for the motor and test zig, Analog Device IC ADXL322 [13] has been selected for the present work. This sensor measures acceleration with a full scale range of 2g (typical). It can also measure both dynamic (vibration) and static acceleration (gravity). The output voltages are proportional to the acceleration.

4.1 Sensor Packaging

In order to provide protection to the basic MEMS sensor with signal conditioning electronics, it is necessary to encapsulate them together in a way such that the complete encapsulated module is easily mountable on the motor where the vibration is to be monitored. To achieve this, a metal casing is designed to house the MEMS sensor, pre-processing signal amplifier connectors etc. Solid blocks of aluminum are used for making different parts of the housing. Broadly, the complete housing is made of three parts and it's detailed engineering drawing is shown in Fig.-6.

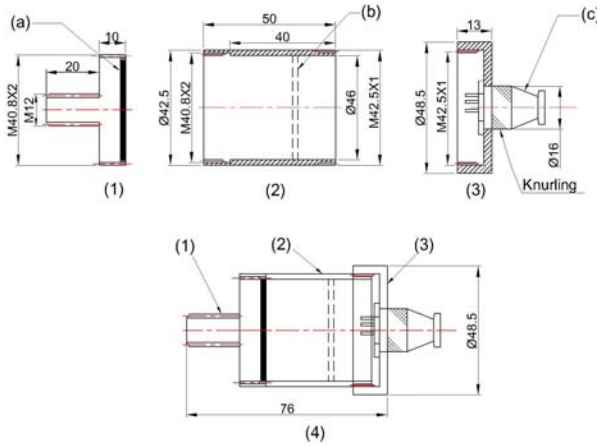

Figure 6: Vibration sensor assembly detail (1) bottom part (2) Main body with signal amplifier card (3) Top part with circular connector, (a) MEMS PCB and (b) amplifier PCB

Different mounting arrangements for the sensor are possible. In the present work, a threaded stud mounting arrangement, as shown in Fig.-6(1), has been considered. This arrangement gives the best contact between the sensor body and the vibrating body with a wide dynamic measurement range for vibration. The basic MEMS sensor is also fitted on this part (marked as 'a'). A rectangular groove is recessed on the inner surface of this block, to provide proper mounting base for the basic MEMS sensor.

Part (2) is the main body in which the preprocessing signal amplifier card is fixed (marked as 'b'). Part (1) and part (c) get attached to the body part (b) through male-female type threading arrangement. Part (a) has male tapered threading whereas part (c) has female tapered threading. This arrangement for coupling of different parts will give an easy access to each component during maintenance. For supply in and for signal out, lightweight threaded - 5pin circular connector (DIN 45322) is used. This connector is fitted in the assembly part (3) and is marked as (c). The complete assembly is shown in Fig.-6(4).

Figure 7: Photograph of MEMS vibration sensor - design and developed for this research work

The photographs of different components of vibration sensor developed for this application are shown in Fig.-7.

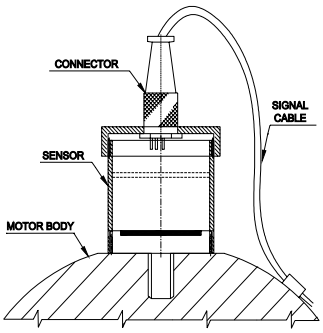

Figure 8: Arrangement drawing of vibration transducers

To reduce the stress on signal cable a provision is made for proper anchoring of the cable, as shown in Fig.-8. The mounting arrangement of the complete sensor on motor is shown in Fig.-8.

4.2 Data acquisition system

A microcontroller based data acquisition board (MC-DAQ) is developed and used here with two objectives:

- To use an independent data acquisition system with data buffering feature to reduce the computational load on the main central fault diagnostic system.

International Journal of Scientific Engineering and Research (IJSER)
www.ijser.in
ISSN (Online): 2347-3878
Volume 2 Issue 9, September 2014

- To have a dedicated hardware that can be installed close to the motor and can sustain the industrial harsh environment.

PIC-18F6520 series microcontroller [19] is used here for developing the DAQ (data acquisition) board. The basic schematic diagram is shown in Fig.-9.

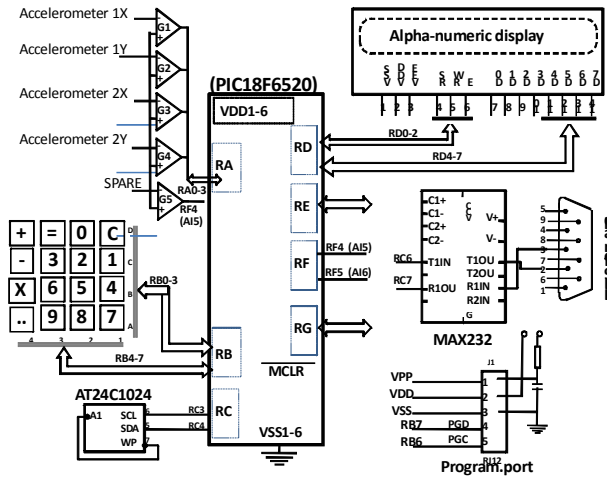

Figure 9: Schematic of microcontroller (PIC-18F6520) based DAQ board developed for this work.

This MC-DAQ scans the data, stores locally and transmits it over serial link to PC using simple ASCII protocol. The data buffering can be done for a maximum of 30secs with a maximum scanning rate of 4kHz for 4 analog input channels. A 4x4 matrix membrane type key pad and a (2line) 16 character LCD display are also provided to make the MC-DAQ board more user friendly.

4.3 Vibration transducer installation

The mounting of vibration transducers needs special attention to faithfully reproduce the vibration of the frame (motor) at the base of MEMS, by avoiding any type of rocking or bending of the transducer. Following steps are followed in this work for creating proper mounting arrangement on motor frame:

1. Flat surface creation on the motor frame above the bearing housing.
2. Milling and then drilling of the pilot hole of 3mm and main drill of 6.9mm perpendicular to the surface. It is essential to prevent any damage to frame which is generally made of cast iron.
3. Drill depth shall be up to 8-10 mm
4. Tap creation in drill with M8 tap sets for tightening the vibration transducers which have stud arrangement.
5. Cleaning of the surface and tightening the sensor into the hole using a torque wrench, keeping in mind the MEMS direction (as discussed above) and maintaining proper contact between the base of the sensor and the mounting surface.

5. Results

The performance of MEMS vibration sensor is evaluated for monitoring the vibration signal and associated frequency components. The tests are conducted for the sensor fitted on 7.5KW induction motor under different operating conditions. In vibration signal analysis, one of the main emphases is to remove the noise and mitigate the unwanted vibration signal (noise) originating from the sensor or other rotating machines (operating in the vicinity) and the target machine. The effectiveness of the noise removal algorithm is checked with a simulated signal. The noise signal, the original signal and the corrupted signals are used to check the performance of the noise removal algorithm, and are shown in Fig.-9 (a, b, c) respectively.

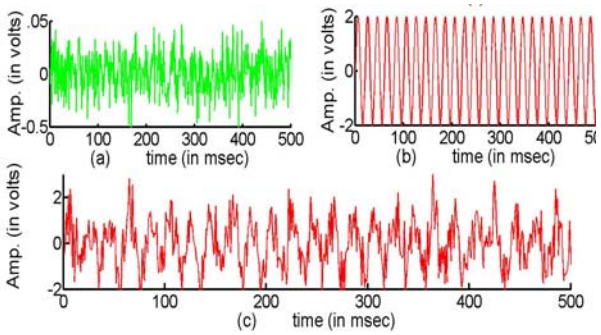

Figure 10: Test signal (a) white Gaussian noise signal, (b) pure sinusoidal wave, (c) signal combining (a) and (b)

The effectiveness of auto-correlation function was examined with different combinations of noise and signal ratio. The frequency spectrum of noisy signal has different peaks, other than the fundamental frequency peak, as shown in Fig.-11 (a). After applying the ACR filter, there is considerable suppression of noise as illustrated in Fig.-11 (b).

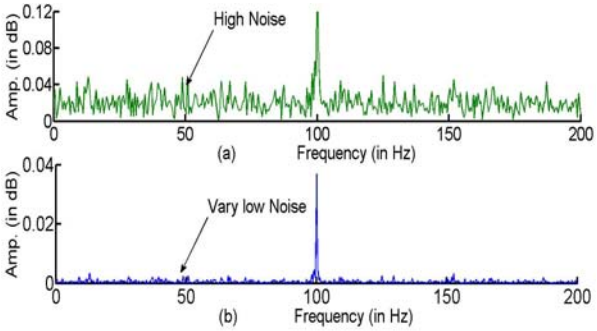

Figure 11: Illustrating the performance of noise removal using auto-correlation function

The application of autocorrelation function for noise removal is further substantiated by applying it on an actual rotating machine (in this case an induction motor). It can be observed in Fig.- 12, that not only the low amplitude frequencies (multiple of rotational frequency and floor noise) are suppressed but the actual signal level has also improved from $7.2X10^{-3}$ g to $11.7X10^{-3}$ g i.e −38dB to −42dB in amplitude.

For each fault, different fault combinations are built up by changing the fault instant or arranging fault sequences, in order

International Journal of Scientific Engineering and Research (IJSER)
www.ijser.in
ISSN (Online): 2347-3878
Volume 2 Issue 9, September 2014

to take into account the random nature of the fault instant. The test results for different simulated faults with usual variability of the signal spectrum are discussed here.

The typical axial and radial vibration spectra for healthy and faulty motors are shown in Fig.-12. The x-axis and y-axis of accelerometer signals are referred to here as axial (along the motor shaft) and radial (radial to stator bore) vibration signal, respectively. It is found that the vibration transducer is capable of capturing these unique frequency peaks.

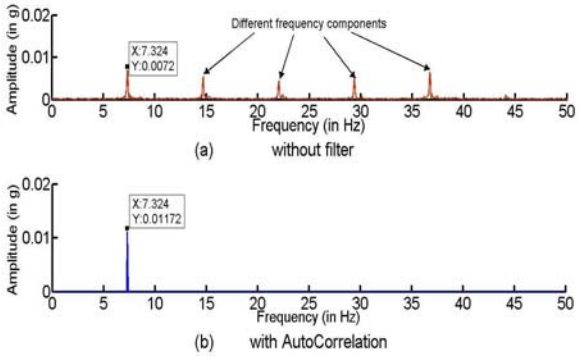

Figure 12: Demonstrating actual vibration signal with and without ACR

A comparative analysis of axial and radial vibration frequency components at different loads and at frequency ($f_r = 12.2Hz$) for healthy conditions are presented in Fig.-13. As expected, the spectral information related to f_r and $2f_r$ for radial signal in the frequency spectrum is seen to be more prominent as compared to that for axial vibration.

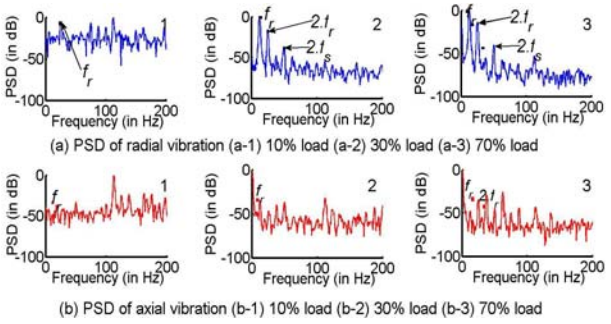

Fig.-13: Typical power spectra of axial and radial vibration signal of the machine rotating at 12.0Hz; under different load conditions.

The experimental investigations on the excited vibration signals of the machines sensed in axial and radial direction are further carried out under different test conditions to ascertain the detectability of fault frequencies. The radial vibration pattern was examined for different values of load torque oscillations) and result is presented in Fig-14.

Unlike symmetric loading of healthy motor, where f_r component is the only prominent factor, load imbalance conditions depend on $2f_r$ components as well. The increase in amplitude of these frequency components for the increase in loading are clearly captured by the new sensor.

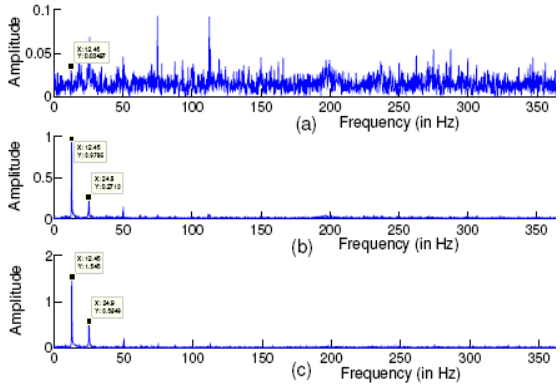

Figure 14: Illustration of radial vibration signal for different oscillatory load with (a) 0.02N-m, (b) 0.042N-m, (c) 0.084N-m

More rigorous tests are carried out to check the ability to detect fault frequencies under combined fault conditions. One such result, for motor with (mixed) eccentricity and motor loaded with an asymmetric load under different operating speeds are shown in Fig.-15. Presence of 1X (f_r) and ($2f_r$) components also indicates the presence of load imbalance.

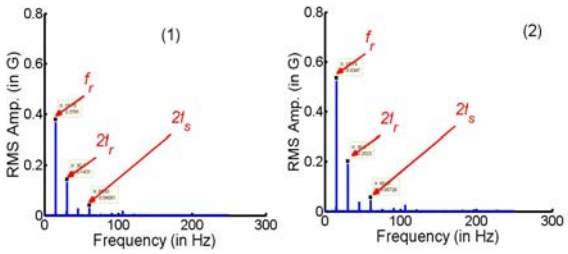

Figure 15: Vibration spectra of a motor with eccentricity and load imbalance condition. (1) mixed eccentricity with Load imbalance 0.0). (1) mixed eccentricity 42N-m (2) Load imbalance 0.084N-m. Both the cases dynamic eccentricity and static eccentricity are 21% and 19.7% respectively.

The typical fault combination like misalignment and load imbalance, widely present in industrial environment (like metal rolling mill) is depicted in Fig.-16.

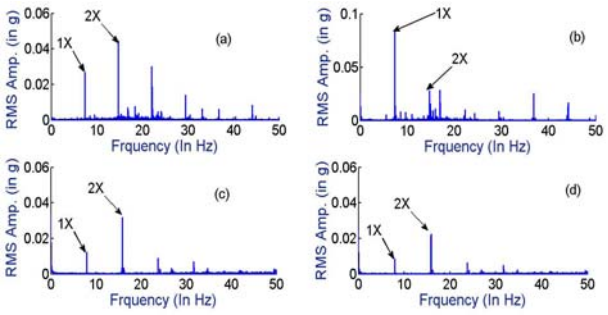

Figure 16: Typical spectral plot of motor vibration for combined fault (misalignment and load imbalance).

The results demonstrate that the 1X and 2X components in axial and radial vibration signal are clearly detectable. The combination of the 1X and 2 X components in axial (Fig.16-a and b) and radial vibration (Fig.16-c and d) indicates the presence of misalignment and load imbalance, as expected.

6. Conclusion

This paper has dealt with the design and the developmental aspects related to a low cost vibration sensor. To improve the characteristic signal detection capability in the acceleration signal, a new noise cancellation algorithm using auto-correlation function and adoptive threshold based filters is developed in this paper.

The potential of the proposed signal processing technique has been assessed under different operating and fault conditions, in order to extract the fault feature frequencies of the weak fault signals in the presence of strong noise. These methods have been proved to be very effective for filtering the periodic, white Gaussian and random noise in real-time acceleration signals.

References

[1] M. E. Elnady, J. K Sinha and S. O. Oyadiji, "Condition monitoring of rotating machines using on-shaft vibration measurement. In: Proceedings of the IMechE, 10th international conference on vibrations in rotating machinery, London, UK, 11–13 September 2012.

[2] A. Muszynska, "Vibrational Diagnostics of Rotating Machinery Malfunctions", International Journal of Rotating Machinery, vol1 Issue 3-4, pp 237-266, 1995

[3] J. K Sinha and K. Elbhbah "A future possibility of vibration based condition monitoring of rotating machines", Mechanical Systems and Signal Processing, vol 34: pp 231–240, 2013.

[4] F. Jiang, W. Li, Z. Wang, and Z. Zhu, "Fault Severity Estimation of Rotating Machinery Based on Residual Signals," Advances in Mechanical Engineering, pp. 1-8, 2012.

[5] N. Tandon and A. Choudhury, "A review of vibration and acoustic measurement methods for the detection of defects in rolling element bearings," Tribology International, vol. 32, pp. 469–480, 1999.

[6] W. R. Finley, M. M. Hodowanec, and W. G. Holter, "An analytical approach to solving motor vibration problems," in IEEE-Ind. Appl. Society, 46th Annual Petroleum and Chemical Industry Conf., Knoxville, TN, 13-15, pp. 217–232, Sept. 1999.

[7] G. Perrone and A. Vallan, "A low-cost optical sensor for noncontact vibration measurements," IEEE Transactions on Instrumentation and Measurement, vol. 58, no. 5, pp. 1650–1656, 2009.

[8] T. K. Gangopadhyay, "Prospects for Fiber Bragg gratings and Fabry-Perot interferometers in fiber-optic vibration sensing," Sensors and Actuators A, vol. 113, no. 1, pp. 20–38, 2004.

[9] J.P Sebastia, J.A. Lluch, J.R. Vizcaino and J.S. Bellon, "Vibration Detector Based on GMR Sensors", IEEE Transactions on Instrumentation and Measurement, vol. 58, no.3, 2009, pp 707-712.

[10] A. Albarbar, S. Mekid, A. Starr, and R. Pietruszkiewicz, "Suitability of MEMS accelerometers for condition monitoring: An experimental study," Sensors (Basel), PMCID: PMC3672998, vol. 8, no. 2, pp. 784–799, 2008.

[11] H.Xie, G. Fedder, "CMOS z-axis capacitive accelerometer with comb-finger sensing". In Proc. IEEE Micro Electro Mechanical Systems (MEMS), 2000; pp. 496-501.

[12] V. Biefeld, A. Buhrdorf and J. Binder, "Laterally driven accelerometer fabricated in single crystalline silicon", Sensor Actuators, vol. 82(1), 149-154, 2000.

[13] J. Sinha, "On Standardisation of Accelerometers". Journal of Sound and Vibration 2005, 286, 417-427.

[14] Analog devices, http://www.dimensionengineering.com/datasheets/ADXL322.pdf.

[15] S. E. Lyshevski, "MEMS and NEMS: systems, devices and structures" CRC Press LLC, USA, 2002.

[16] H. Luo, G. Fedder, and L. Carley, "A 1 mg lateral CMOS-MEMS accelerometer," Proceedings IEEE Thirteenth Annual International Conference on Micro Electro Mechanical Systems, 2000.

[17] Yazdi, N.; Ayazi, F.; Najafi, K. "Micromachined inertial sensors", Proc. IEEE, Vol.86, no. 8, pp. 1640-1659, 1998.

[18] F. Mohn-Yasin, C. E. Korman, and D. J. Nagel, "Measurement of noise characteristics of MEMS accelerometers," Solid-State Electronics, vol. 47, pp. 357–360, 2003.

[19] Microchip, PIC18F6520/8520/6620/-- Data Sheet", http://www.datasheetarchive.com/PIC18F6520-8520-datasheet.html